JOURNAL OF OPTOELECTRONICS AND ADVANCED MATERIALS Vol. 12, No. 2, February 2010, p. 360 - 364

Optimization of the threshold voltage of an image intensifier in ultra-fast photocathode gating

TINGYI GU, ZHENXING HAN, KAN WU, JIANPING CHEN
State Key Lab of Advanced Optical Communication Systems and Networks, Department of Electronic Engineering, Shanghai Jiao Tong University, Shanghai, China, 200240

In this paper, the spatial distortion of the gated image intensifier is investigated theoretically. A software model is presented and simulations are performed. The accuracy of the model is verified by the broadband frequency response alignment to the measurement. The correspondent simulation result in the time domain is evaluated by two criteria, uniformity and noise to signal ratio. Both criteria show that the non-uniformity caused by the electric field distortion can be minimized by applying a suitable threshold for input pulse shaping.

(Received May 28, 2008; accepted February 18, 2010)

Keywords: Image intensifiers, Threshold voltage, Fast gate, Uniformity index, Noise to signal ratio

1. Introduction

Ultra-fast gating image intensifiers have wide applications in biotechnology, industry, electronics and astronomy, such as hypervelocity impacts, short time physics, ballistics and combustion imaging [1, 2]. The basic operations of the image intensifiers can be described as follows: An incident photon is absorbed by the photocathode and converted to an electron, then the electron is accelerated between the photocathode and micro-channel plate (MCP) gap by an external applied voltage. Furthermore, the accelerated electron enters one channel of the MCP and gets multiplexed into thousands of electrons due to the process of secondary electron emission. Those electrons exiting the MCP will be accelerated again toward the phosphor layer and converted back to one light spot in the screen [3,4]. So, the quality of an image will be affected by lots of factors, such as photo-absorption in photocathode, electron acceleration, electron multiplication in MCP, etc. Each of them contributes to the image spatial distortion, which is evaluated by signal to noise ratio. Most of those factors have been studied previously [5-8]. However, the effect of the transient electrical field across the gap between photocathode and MCP for threshold controlling is still not quite clear. For a gated image intensifier, a high voltage pulse will be used to control the gating process, so the transient response of the gated image intensifier is essential. The device is so complex that it is unlikely analytic methods or common intuition could usefully be applied. In this paper, we will investigate image non-uniformity caused by the electric field distortion by CST microwave studio [9]**.** In section 2, we present the model of the image intensifier. It is followed by the simulation result in section three. In section four, we address the issue of the relationship between the nonuniform transient field and the image performance. All results are discussed and analyzed.

2. Basic structure

Fig. 1 (a) shows the basic structure of the intensifier. Part 1 is the input window made of glass or a fiber optic plate. It is deposited with light-sensitive material as the photocathode (part 2). Part 3 and part 4 are conductive films on MCP (part 5) front and rear surfaces. Part 6 is a phosphor layer deposited on the output window (part 7) made of glass. Based on the schematic structure, Fig. 1 (b) describes the practical structure connected to the electric control signal generation. The connection is composed of five silver rings. The function of the first ring on substrate is to connect the photocathode to the inner wire of coaxial cable. The metal shield of coaxial cable is linked to the MCP front face by the second ring on the MCP front surface. The rest of the rings are designed to connect to the ground or the constant voltage source. They are involved in the simulation structure because of the coupling effect between those metallic plates.

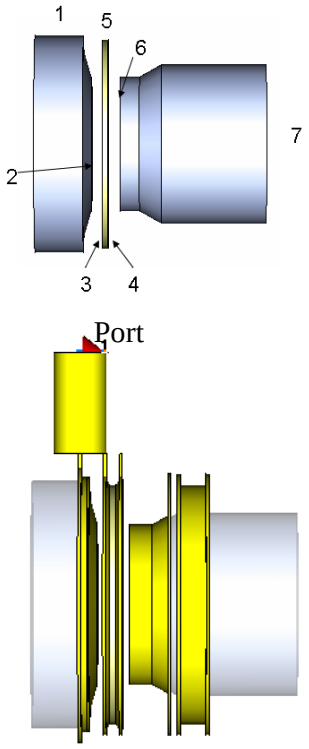

(a) Schematic structure (b) Simulation structure

Fig 1. Image intensifier structure.

We use CST Microwave Studio® to analyze the structure [9]. Free space is taken as the boundary. The excitation signal used is a Gaussian pulse with a 0.5ns rising edge launched into the coaxial cable from the electrical port shown in Fig1 (b). Table 1 lists the main parameters used in this model.

Table 1. Device Dimensions in Fig. 1 (a) [11-13].

	Component	Material	Epsilon	Conductivity
1	Input Window	Glass	2.1	-
2	Photocathode	CsI (T1)	10.4	$4.6*10^{6}$(S/m)
3,4	MCP high conductive surfaces	Nicrome	-	$2.2*10^{5}$(S/m)
5	MCP	Lead Glass	-	$1.0*10^{-8}$(S/m)
6	Phosphor	Phosphor	4	-
7	Output Window	Glass	2.1	-

The validity of the model was verified by comparing the simulated and experimental S-parameters in a wide frequency range, because the S-parameters are unique for each specific element. The comparing frequency range was set from 1 to 6 G Hz.

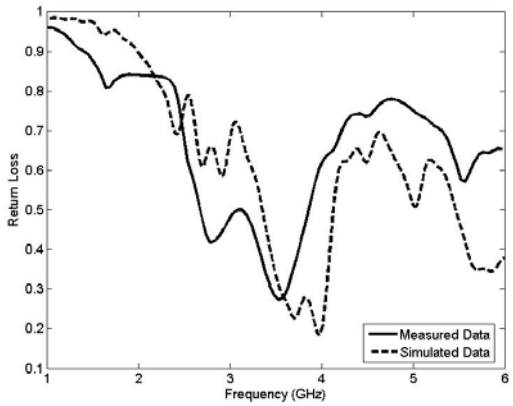

Fig. 2. Simulated and measured return loss (solid line is the measurement result, and the dash line is for the simulated result, the frequency range is from 1-6GHz.)

The experimental and simulation results are very close as shown in the Fig. 2. The device's return loss was measured by the Agilent 8722ES S-parameter Network Analyzer. The simulated and measured results exhibit the same peaks at 1.5, 2.8, 3.5 and 4.5 GHz, which verify the rightness of the simulated model.

3. Image performance evaluation

Fig. 3 shows the time domain simulation results. The electric field distribution between the photocathode-MCP gap changes with time. Fig. 3 (a) displays the distribution in the entire area, providing the peak of gating pulse input is 200V. The color in the middle circle is especially bright, which means the high electric energy concentration in the field of view (FOV), a circular area with 12 mm radius. The electric field distribution in the FOV is not uniform as shown in Fig. 3 (b). The Z-component of the electric field near the edge is more intensified than in the centre as shown in Fig. 3 (c) (d). This behavior stays the same for most of the time. The contradiction is especially obvious when the electric field reaches maximum, which takes place at 1.3ns in Fig. 3 (c) and (d). Both of these fig.s show the evolution of the electric field at different points in the FOV.

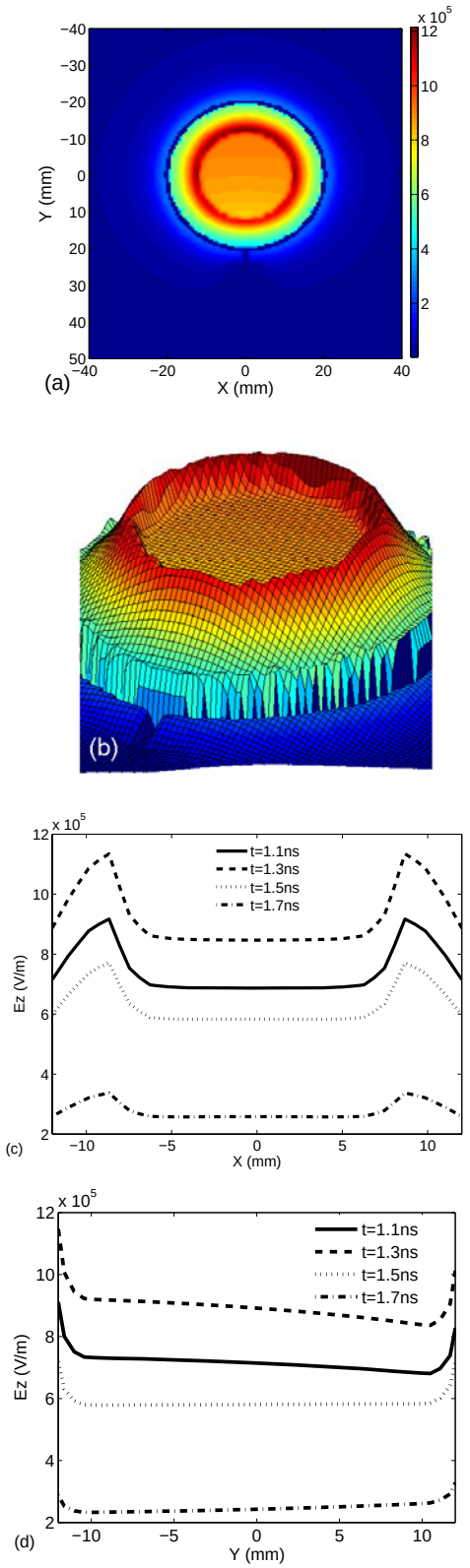

Fig. 3. Simulated Z component electric field distributions in the photocathode and MCP gap: (a) in the full area, t=1.2 ns (b) in the field of view, t=1.2 ns, (c) at y=0 and (d) x=0 (for four different times at 1.1ns, 1.3ns, 1.5ns and 1.7ns, respectively).

The gating is accomplished with a time- and space-varying electric field. The threshold voltage is the constant bias voltage added on the front conductive face of MCP for preventing the electrons passing through the photocathode and MCP gap when there is no gating pulse in. The local pixel is ON when the absolute voltage on the photocathode is above the threshold. The difference in response indicates that the ON/OFF status is different from one pixel to another. However, the difference does not have any effect on the overall gain [12]. Such phenomenon can be described by the parameter of uniformity index defined is [14] as:

$$U = \frac{N_{\max} - N_{\min}}{N_{\max} + N_{\min}} \times 100\% \tag{1}$$

where N_{max} and N_{min} are the maximum and minimum numbers of the pixels of the "ON" area, respectively. In particular, when the uniformity index is calculated for the entire FOV, the number of counted photons, N, only depends on the time duration in which the voltage is above threshold [15, 16]. Each pixel, defined as a little square, is so small that the electric distribution is supposed to be uniform throughout and, hence, can be used to depict the two dimensional plane into discrete squares. Provided all the other conditions are ideal, the integral uniformity is only disturbed by transient electric distribution, i.e., nonuniform bias voltage. If the bias voltage is big enough, the output photoelectrons can emit the surface of photocathode, according to the following relationship:

$$\varphi = qV_{bias} - E_{cutoff} \tag{2}$$

where the cutoff energy is a constant, and φ is kinetic energy of output photoelectron. The output kinetic energy depends on the photocathode thickness and material it used [17]. When φ is positive, the local area, or pixel is 'ON'. Since N is the account of ON pixels, we have

$$N = \rho \times S \times v \times t_{ON} \tag{3}$$

Where ρ is the mean density of the electrons coming out of the photocathode, S is the area of pixels, and t_{ON} is the time duration of "ON" status at the sample point. Under ideal condition, v is the mean velocity of the electrons emitting out of photocathode, and since the intensity of light is uniform on the input surface and so the photon count is the same for all the pixels. So the uniformity index is obtained by substituting Eq. (3) into Eq. (1).

$$U = \frac{t_{\max} - t_{\min}}{t_{\max} + t_{\min}} \times 100\% \tag{4}$$

where $t_{\max}$ and $t_{\min}$ are the maximum and minimum time duration when the local field is above threshold. Suppose there are n pixels in FOV, so the average signal is defined as:

$$\overline{S} = \frac{1}{n}\sum_{i=1}^{n} N_i \tag{5}$$

where N_i is the signal intensity on pixel i. The noise is evaluated as:

$$\sigma^2 = \frac{1}{n}\sum_{i=1}^{n}(N_i - \overline{N})^2 \tag{6}$$

The noise to signal ratio is defined as:

$$N/S = \frac{\sqrt{\sigma^2}}{\overline{S}} \tag{7}$$

When the Image Intensifier works under the temporally gate (i.e., shutter) mode, a low uniformity index or low N/S means a good performance.

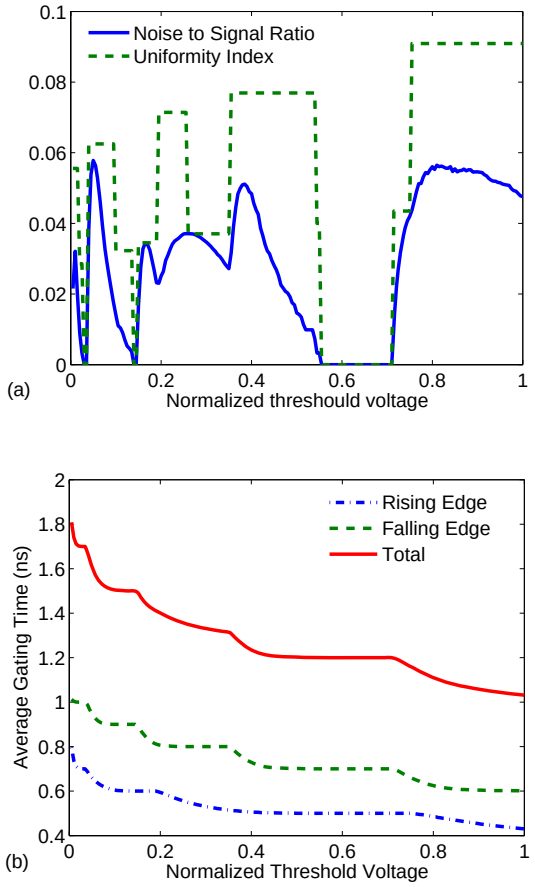

Fig. 4 criteria versus threshold voltage (a) noise to signal ratio and uniformity index versus normalized threshold voltage (b) Average gating times of the pixels in sensitive area for rising edge, falling edge and total.

Fig. 4 (a) exhibits the uniformity index and noise to signal ratio under different threshold voltages according to Eq. (4) and Eq. (7). With almost the same trend, the two criteria are consistent. The uniformity index and noise to signal ratio are zero when the normalized threshold voltage is 0.035, 0.14 and in the range from 0.56 to 0.71. Theoretically if the threshold voltage is set at those values, the electric distortion can be totally avoided. It is not surprised because the counterpropagating waves integrates in the capacidance like structure and the uniformity can be achived.

The threshold voltage also adjusts the averange gating time. With higher threshold voltage, the average gating time decreases and gating speed is higher as shown in fig. 4 (b). The total gating time is 1.7 ns and 1.5 ns for threshold voltage at 0.035 and 0.14 respectively. When the normalized threshold voltage is in the range from 0.56 to 0.71, the total gating time is 1.2 ns.

Low threshold causes higher sensitivity to background radiation or thermal noise. High threshold voltage brings about less gating time, but it also means longer transient time for the photoelectrons passing through the photocathode-MCP gap and thus leads to larger lateral expansion.

3. Conclusion

We simulate the transient electric field distribution in image intensifier under gating mode. First, the numerical model was verified by comparing the return loss over a wide frequency range with measured data. The device performance was quantified by using the uniformity index and noise to signal ratio. The simulation results depict that complete uniformity can be obtained when the threshold voltage is in some specific ranges. The average gating time decreases with higher threshold voltage. The optimized normalized threshold voltage is 0.14 by taking both gating time and lateral expansion into consideration.

Acknowledgement

The paper is partially sponsored by NSFC (90704002), 863 Project (ID2006AA01Z242 and 2007AA01Z275), Dawn Excellent Scholar Program by Shanghai Municipal Education Commission and the key disciplinary development program of Shanghai (T0102). The authors thank Center for Microwave and RF Technologies for help in S-parameter measurement and beneficial discussions.

References

[1] Hand book of Image intensifiers, Hamamatsu. Available at: http://jp.hamamatsu.com/resources/products/etd

[2] 12bit ultra speed intensified imaging, CooKe. Available at: http:// www.cookecorp.com/

download/?url=%2Fdata%
2FBR_HPE_TCC_0502.pdf
[3] J. P. Estrera and M. Saldana, Proceedings of the SPIE 5079, 2003, p. 212-221.
[4] Fundamentals of high performance CCD imaging, imaging intensification. Available at: http://www.roberscintific.com
[5] M. R. Carter, B. J. McKinley, K. G. Tirsell, Physics Scripta **41**, 390(1990).
[6] W. F. Krolikowski, W. E. Spicer, Phys. Rev. **185**, 882 (1969).
[7] M. Cardona, L. Ley, Photoemission in Solids I, Topics in Applied Physics 26 (1978), Springer, Berlin
[8] K. L. Jensen, P. G. O'Shea, D. W. Feldman, N. A. Moody, J Appl. Phys. **99**, 124905 (2006).
[9] CST microwave studio 2006. CST. Available at: \ http://www.cst.com
[10] E. Shefer, A. Breskin, T. Boutboul, R. Chechik, B. K. Singh, H. Cohen, I. Feldman, Phys. Rev **92**, 8, (2002).
[11] Hand book of MCP Image Intensifier. Photek. Available at: http://www.Photek.co.uk.
[12] J. L. Wiza, Nuclear Instruments and Methods, **162**, 587 (1979).
[13] B. R. C. Garfield, Brit J Appl. Phys. **17**, 1005, (1966).
[14] Burle Electro-Optics, Inc., POB 1159, Sturbridge, MA 01566, Available at: http://www.burle.com.
[15] G. Muehllehner, T. Wake, R. Sano, J. Nucl. Med. **22**, 72 (1981).
[16] NEMA Standards Publication NU 1-2007, Performance Measurements of Gamma Cameras.
[17] M. Tenhunen, J. Pyykkonen, M. Tenhunen-Eskelinen, K. Jaatinen, J T Kuikka, Phys. Med. Biol. **41**, 1209, (1996).

*Corresponding author: tingyi.gu@gmail.com